

Supplementary Materials

Methods.

Waters and metals. Density for the α I MIDAS and β I ADMIDAS metals was clearly visible. Although separate density for water molecules is not present at the resolution obtained, waters were included near these metals when they were in density, or when they improved the geometry of metal – protein coordination during refinement. Density was present for metals in the β -propeller Ca^{2+} -binding β -hairpin loops; although this density was not separate from that for surrounding metal-coordinating residues, metals were included, because otherwise metal-coordinating oxygens came too close to one another after refinement.

Results.

The genu. The connection between the thigh and the genu differs markedly in conformation in α_X compared to α_{IIb} and α_V and helps account for the closer interaction between the thigh and calf-1 domains in α_X . The five residues in the thigh domain preceding the genu, where the conformational differences occur, have a different consensus sequence in α_X and other α I domain integrins than in α_{IIb} and α_V and other Arg-Gly-Asp binding integrins (Fig. S5a), suggesting that the differences in thigh/calf-1 orientation between α_X and α_{IIb} described here are characteristic for these classes of integrins. Mutations of the genu in the α_L -subunit, including Ca-binding residues, decrease exposure of activation-dependent epitopes and decrease ligand binding (Fig. S5b,c), suggesting that these mutations stabilize the bent conformation. These findings

suggest that Ca binds with higher affinity to the extended genu than the bent genu of α I integrins, and are consistent with the lack of a Ca-binding conformation of the genu found here in crystals. Antibodies that recognize the active state of $\alpha_L\beta_2$ map to residues buried on the thigh domain by the calf-1 domain (Fig. 2a,b); furthermore, binding of these antibodies also requires Ca^{2+} and is disrupted by mutation of putative Ca-binding residues in the genu (Xie et al, 2004).

The headpiece and Lys finger. In the headpiece of $\alpha_X\beta_2$, the β -propeller domain and β I domain associate over an extensive interface with an inter-domain orientation essentially identical to that in $\alpha_{Iib}\beta_3$. The β -propeller has seven β -sheets or blades tightly packed together around a pseudosymmetry axis. The β_2 I domain caps one hub of the β -propeller. Although the interfaces are overall similar, in $\alpha_X\beta_2$ compared to $\alpha_V\beta_3$ (Xiong et al, 2001) and $\alpha_{Iib}\beta_3$ (Zhu et al, 2008), a Lys rather than an Arg finger inserts into the β -propeller pseudosymmetry axis, and interactions of the fingertip residue with hub residues are less extensive (Fig. S7).

Supplementary Figure Legends

Figure S1. Structure-based sequence alignments. **a**, alignment of α_X with α_{11b} (Zhu et al, 2008) and α_V (Xiong et al, 2004). **b**, Alignment of β_2 with β_3 (Zhu et al, 2008).

Domains were separately superimposed using SSM (Krissinel & Henrick, 2004).

Structurally equivalent residues are in upper case and otherwise in lower case. Residues absent from structures are in italics. α or 3_{10} -helices are highlighted in cyan and β -strands in pink.

Figure S2. Ectodomain constructs and all class averages from negative stain EM. **a**,

Schematic of integrin $\alpha_X\beta_2$ ectodomain constructs with a C-terminal linker containing a TEV protease cleavage site and a coiled-coil. **b**, Schematic of integrin $\alpha_X\beta_2$ ectodomain

constructs with an additional disulfide bond between GCG sequences following the ectodomain C-termini and preceding the linker. **c**, $\alpha_X\beta_2$ construct as in **b** with C-terminal

GCG disulfide and coiled-coil. **d**, $\alpha_X\beta_2$ construct with C-terminal coiled-coil as in **a**. **e**,

The same construct as in **b** and **c** with TEV cleavage to remove the C-terminal coiled-

coil. **f**, The same construct as in **a** and **d**, with TEV cleavage to remove the C-terminal coiled-coil.

Figure S3. Superpositions of domains. **a**, Relative orientation between Calf-2 domain and β -tail domain. The two domains from 10 $\alpha_X\beta_2$ molecules are superimposed on Calf-2 domain. **b**, superposition of the $\alpha_X\beta_2$ α I domain and the isolated α_X I domain (Vorup-Jensen et al, 2003), both of which show the closed conformation.

Figure S4. Superpositions of $\alpha_X\beta_2$ and $\alpha_{IIB}\beta_3$ on their calf-2 domains, and the CD loop of the β -tail domain. These superpositions emphasize the markedly different orientations of calf-2 in these integrins. In the orientations in a-c, the calf-2 domain is oriented so that its base would be approximately parallel to the plasma membrane, as a surrogate for orientation on the cell surface. **a**, $\alpha_X\beta_2$ and **b**, $\alpha_{IIB}\beta_3$ structure superimposed on calf 2. In **c**, $\alpha_{IIB}\beta_3$ is rotated about 50° in the vertical axis of the page relative to **b**, revealing an overall orientation more similar that of $\alpha_X\beta_2$ in **a**. **d-e**, views of **a** and **b** after rotation in the horizontal axis of the page, to show a bird's eye view looking down on the cell surface, and the significant differences in $\alpha_{IIB}\beta_3$ and $\alpha_X\beta_2$ orientation. **f-g**, The β subunits of $\alpha_X\beta_2$ (**f**) and $\alpha_V\beta_3$ (Xiong et al, 2004) (**g**), in identical orientations after superposition on the β -tail domain. The β 6-strand and α 7-helix of the β I domain (red) are close to the β tail domain CD loop in β_3 and not in β_2 .

Figure S5. The sequence at the genu and effect of mutation of putative genu Ca^{2+} -coordinating residues. **a**, Sequence alignment of human integrin α subunits around the genu. The disulfide-linked genu cysteine residues are highlighted in yellow. **b-c**, Effect of mutating putative genu Ca^{2+} -coordinating residues Asp-749 and Glu-787 in $\alpha_L\beta_2$. **b**. Effect on KIM127 and m24 activation epitope exposure. HEK 293T transient transfectants expressing WT or mutant $\alpha_L\beta_2$ in medium containing 1mM $CaCl_2$ /1mM $MgCl_2$ or 2mM $MnCl_2$ were stained with KIM127 or m24 mAbs and subjected to immunofluorescence flow cytometry. Expression of the activation-insensitive mAb MHM24 was not affected by $MnCl_2$. Data shows specific mean fluorescence intensity as

a percentage of MHM24-specific mean fluorescence intensity, and error bars represent the SD of three independent experiments. **c**, Effect of $\alpha_L\beta_2$ genu Ca^{2+} binding site mutations on cell adhesion. Binding of fluorescently labeled HEK 293T transfectants to immobilized ICAM-1 was as described (Lu & Springer, 1997). Briefly, ICAM-1-IgG Fc fusion protein at 10 $\mu\text{g/ml}$ was immobilized on microtiter plates and blocked with 2% BSA. Binding of ICAM-1 was determined in HBS-BSA buffer (20mM Hepes, pH 7.5, 140 mM NaCl, 2 mg/ml glucose, 1% BSA) in the presence of divalent cations and/or activating antibody CBR LFA1/2 (10 $\mu\text{g/ml}$) or EDTA (5 mM) as indicated. After incubation at 37 °C for 30 min, unbound cells were washed off, and bound cells were quantitated.

Figure S6. Sequence alignment. **a**. Sequence alignment of human αI integrin α subunits around the αI C-linker. The $\alpha 7$ helix of the αI domain is indicated above the sequence. The invariant Glu (E) is highlighted in cyan. **b**. Sequence alignment of α_X , α_M , α_D , and α_L around the linker between Calf-2 domain and TM domain.

Figure S7. β -Propeller/ βI domain interface. **a**. Side view of the Arg or Lys finger of the βI domain and surrounding β -propeller domain residues. **b**, Top view. $\alpha_X\beta_2$ residues are colored in cyan, $\alpha_V\beta_3$ in silver and $\alpha_{\text{Ib}}\beta_3$ in yellow.

References

- Krissinel E, Henrick K (2004) Secondary-structure matching (SSM), a new tool for fast protein structure alignment in three dimensions. *Acta Crystallogr D Biol Crystallogr* **60**(Pt 12 Pt 1): 2256-2268
- Lu C, Springer TA (1997) The α subunit cytoplasmic domain regulates the assembly and adhesiveness of integrin lymphocyte function-associated antigen-1 (LFA-1). *J Immunol* **159**: 268-278
- Vorup-Jensen T, Ostermeier C, Shimaoka M, Hommel U, Springer TA (2003) Structure and allosteric regulation of the $\alpha_x\beta_2$ integrin I domain. *Proc Natl Acad Sci U S A* **100**: 1873-1878
- Xie C, Shimaoka M, Xiao T, Schwab P, Klickstein LB, Springer TA (2004) The integrin α subunit leg extends at a Ca^{2+} -dependent epitope in the thigh/genu interface upon activation. *Proc Natl Acad Sci U S A* **101**: 15422-15427
- Xiong J-P, Stehle T, Diefenbach B, Zhang R, Dunker R, Scott DL, Joachimiak A, Goodman SL, Arnaout MA (2001) Crystal structure of the extracellular segment of integrin $\alpha_v\beta_3$. *Science (New York, NY)* **294**(5541): 339-345
- Xiong JP, Stehle T, Goodman SL, Arnaout MA (2004) A novel adaptation of the integrin PSI domain revealed from its crystal structure. *J Biol Chem* **279**: 40252-40254
- Zhu J, Luo BH, Xiao T, Zhang C, Nishida N, Springer TA (2008) Structure of a Complete Integrin Ectodomain in a Physiologic Resting State and Activation and Deactivation by Applied Forces. *Mol Cell* **32**(6): 849-861

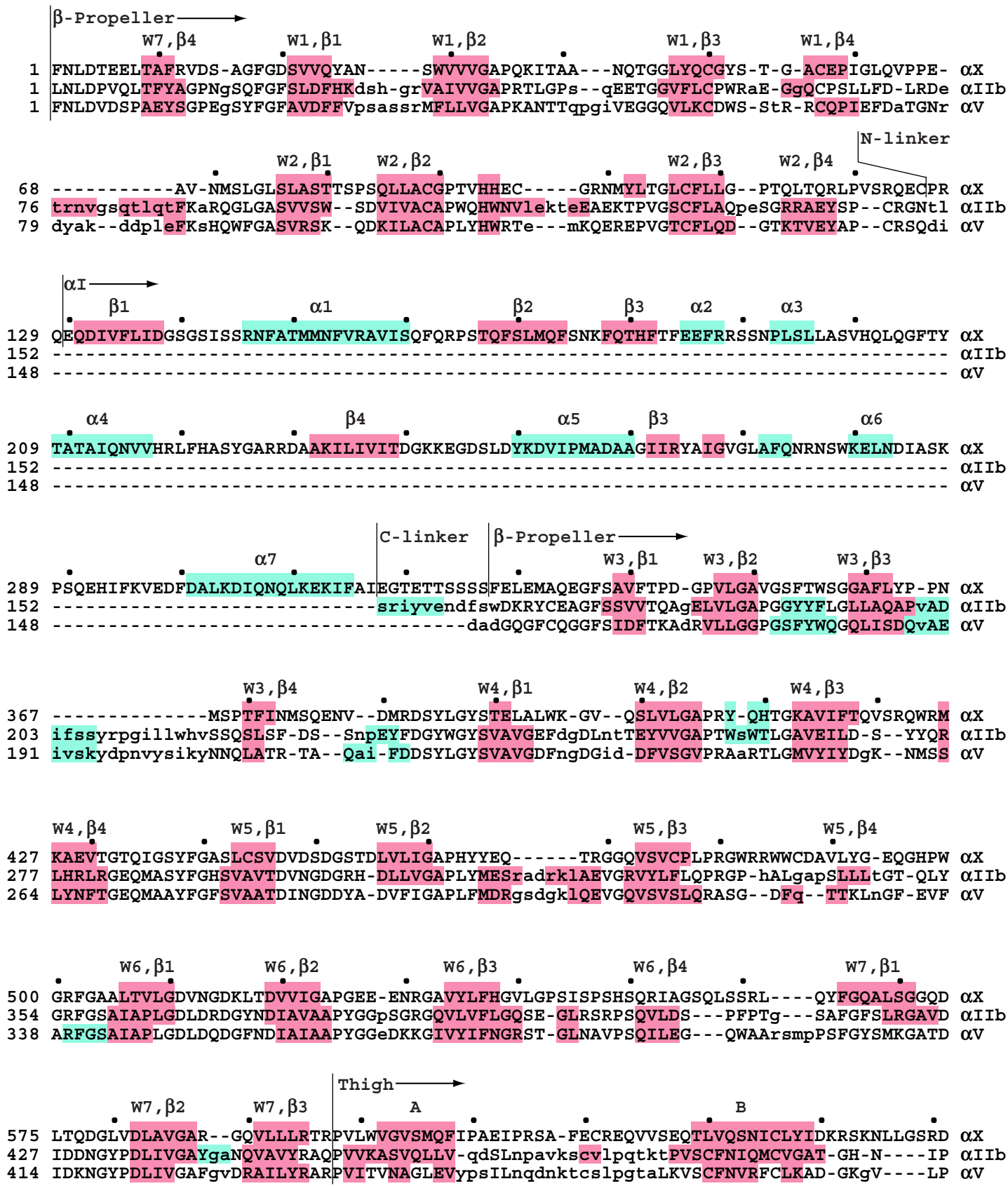


Fig. S1a_p1

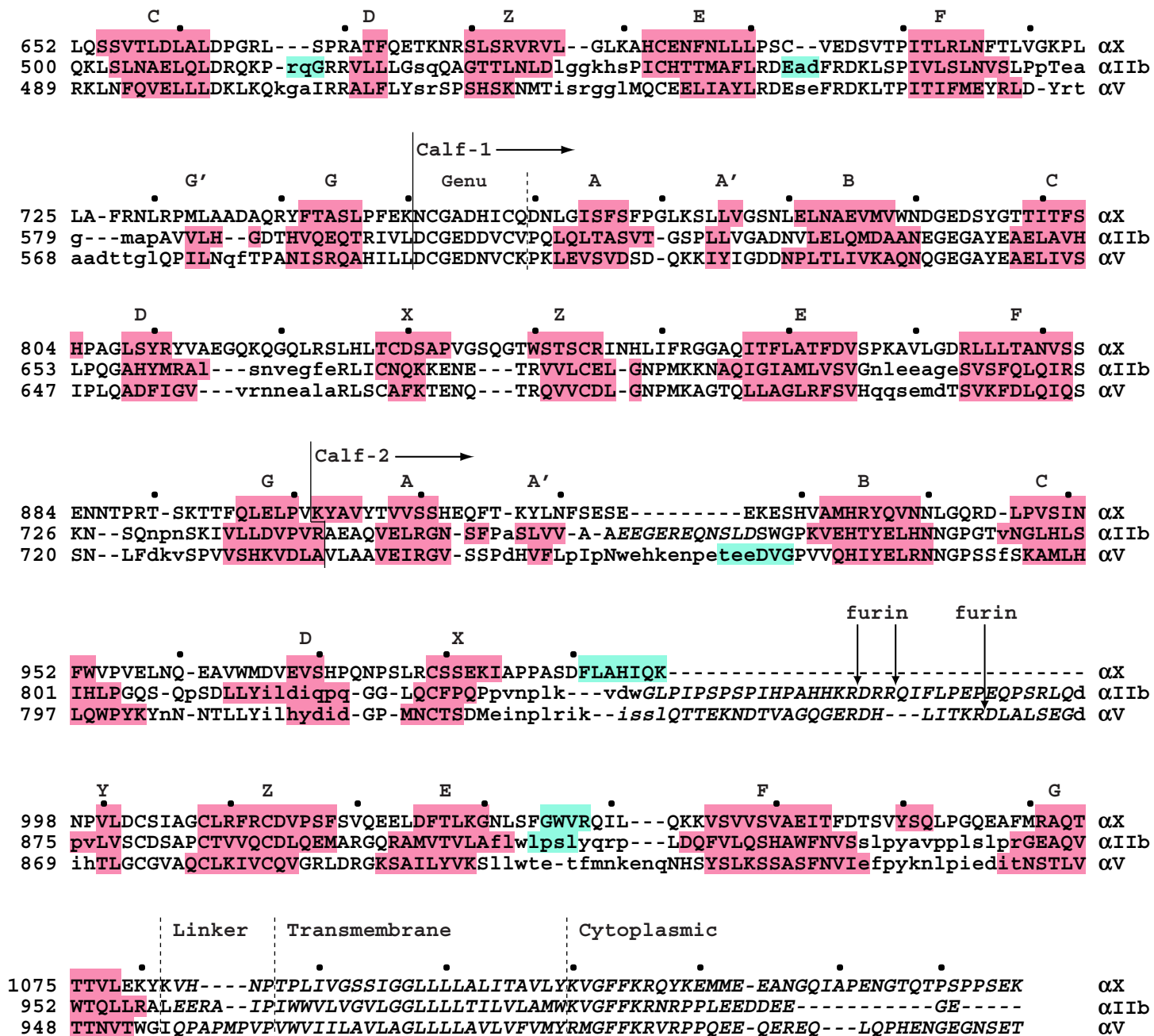


Fig. S1a_p2

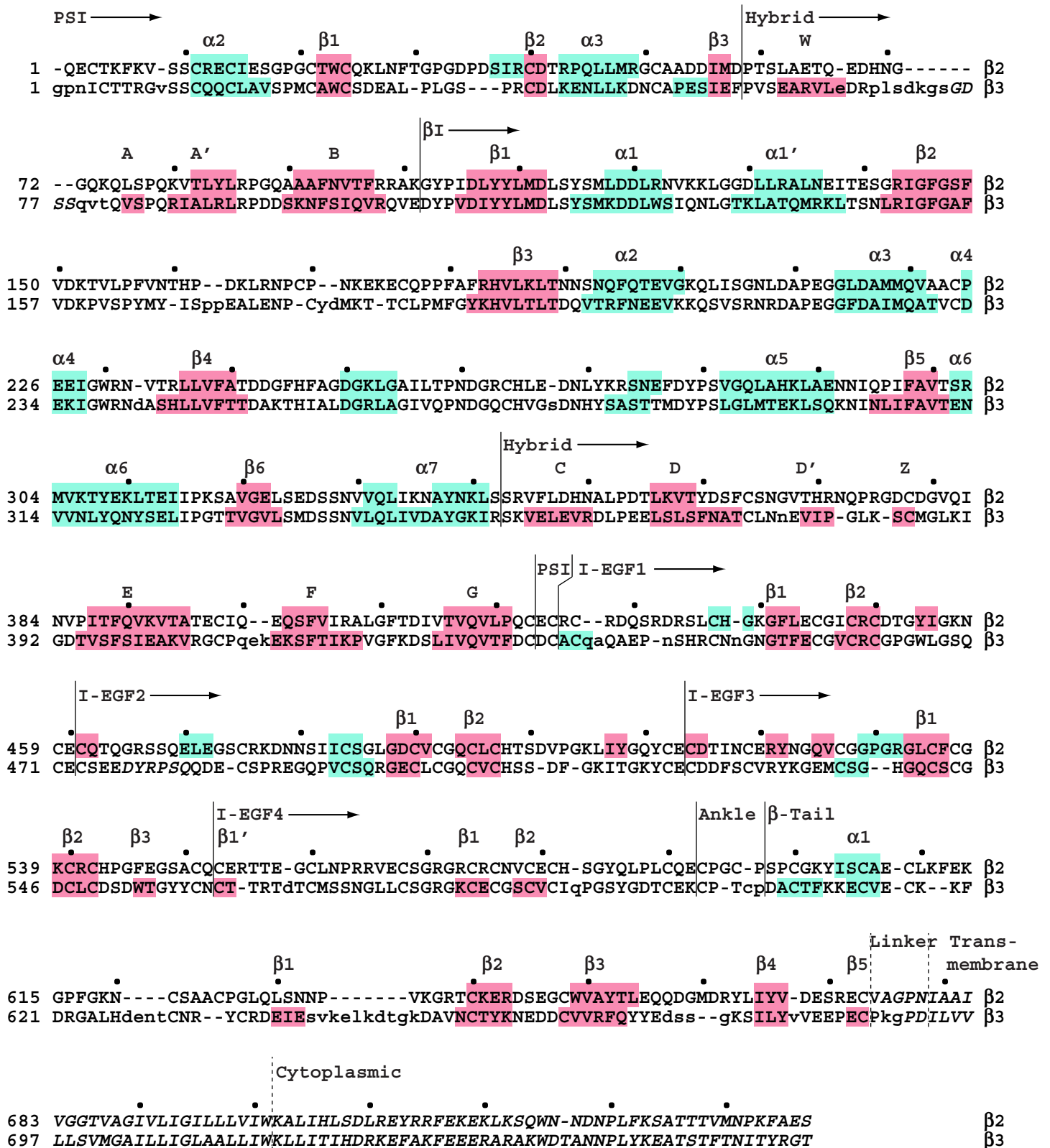
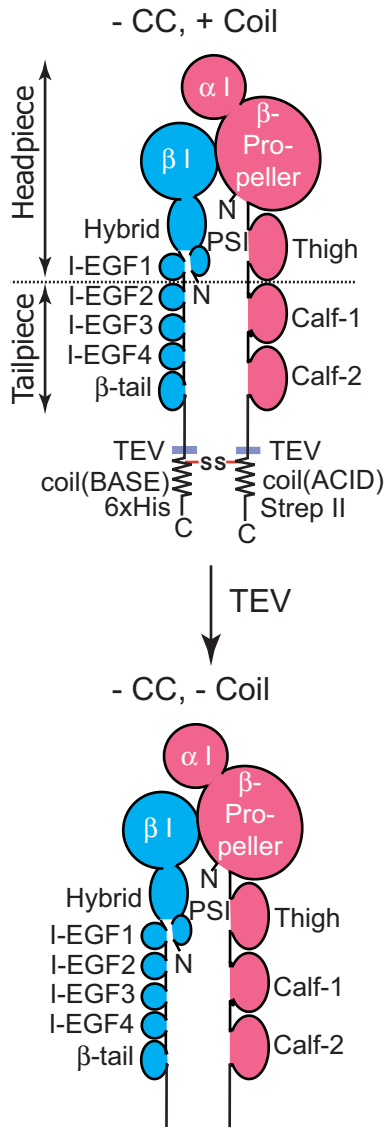
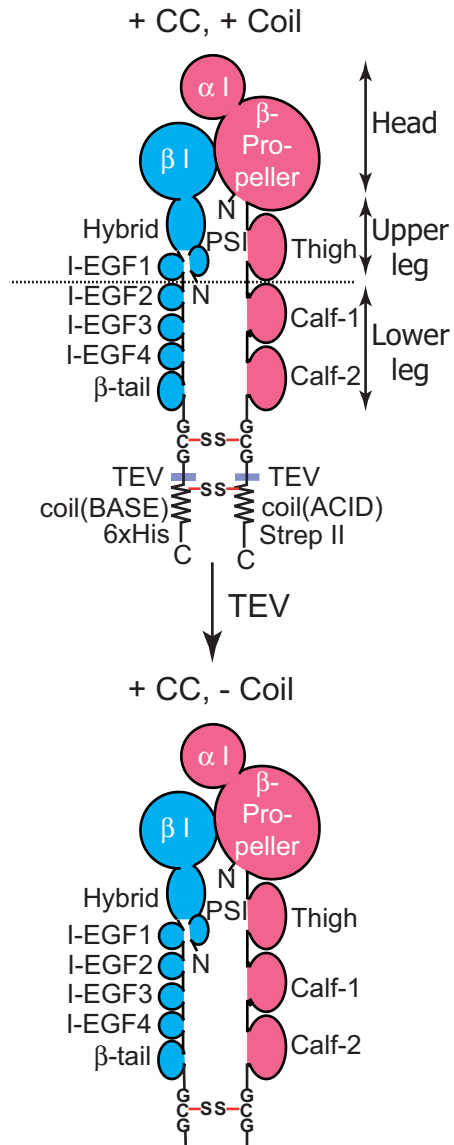
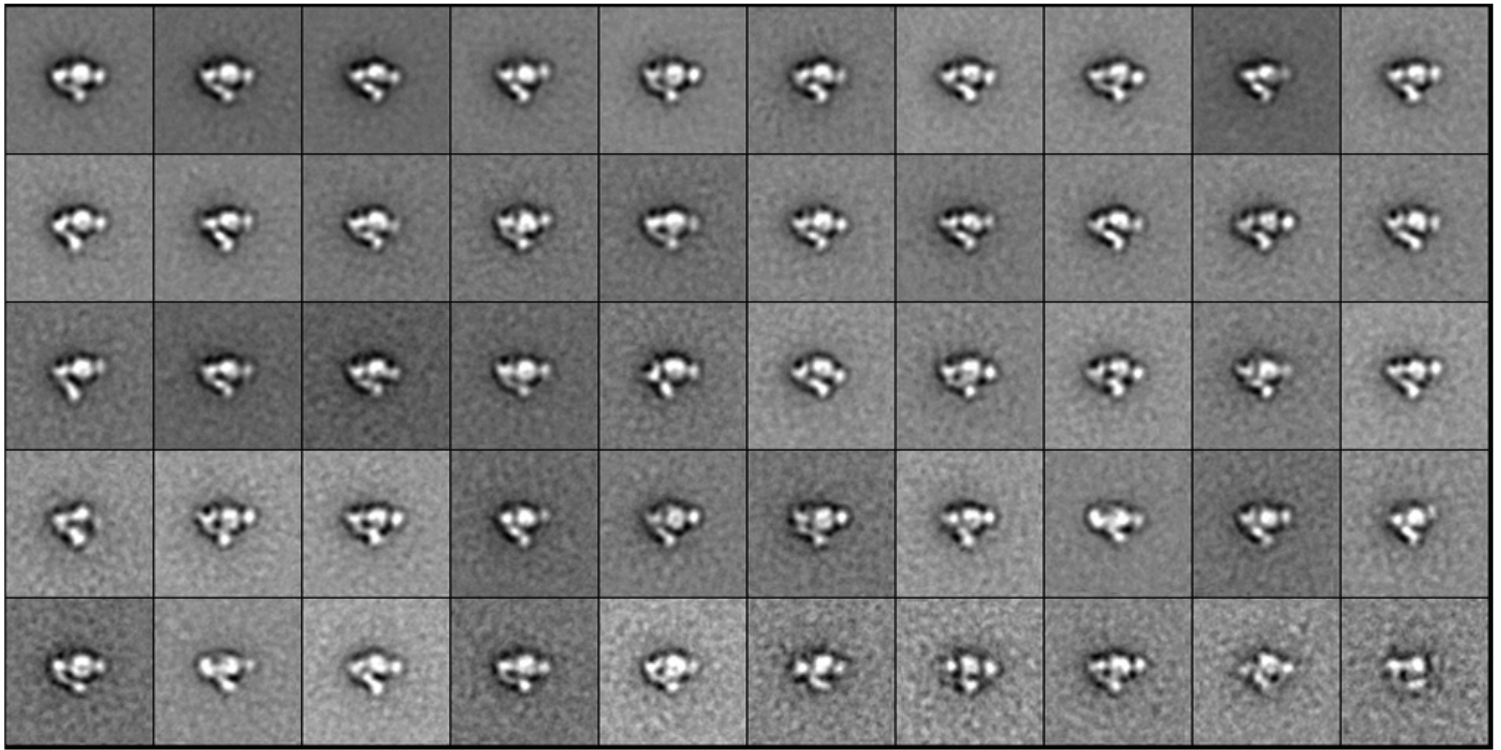


Fig. S1b

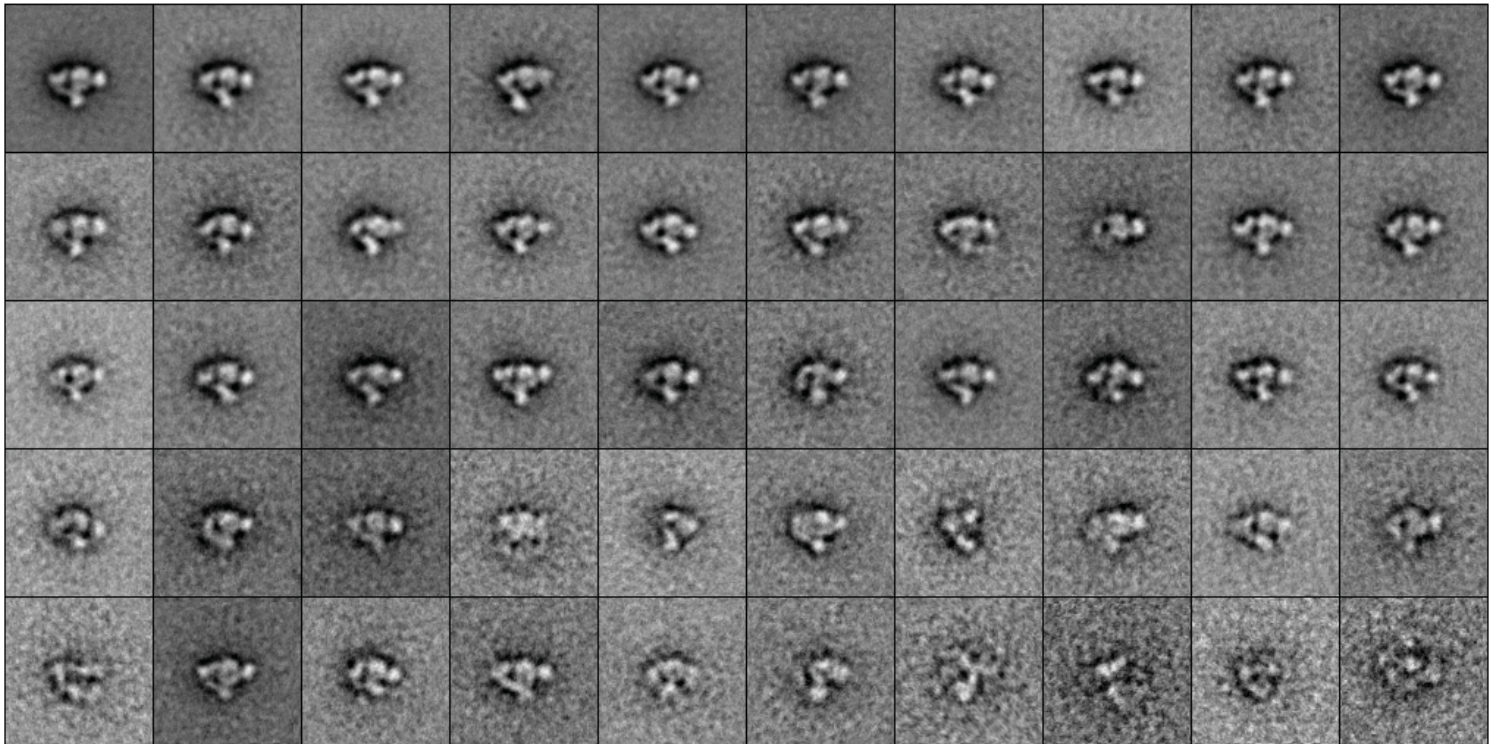
a**b****Fig. S2a, b**

c Class average of $\alpha_x\beta_2$ (+ CC, + Coil)



20 nm

d Class average of $\alpha_x\beta_2$ (- CC, + Coil)

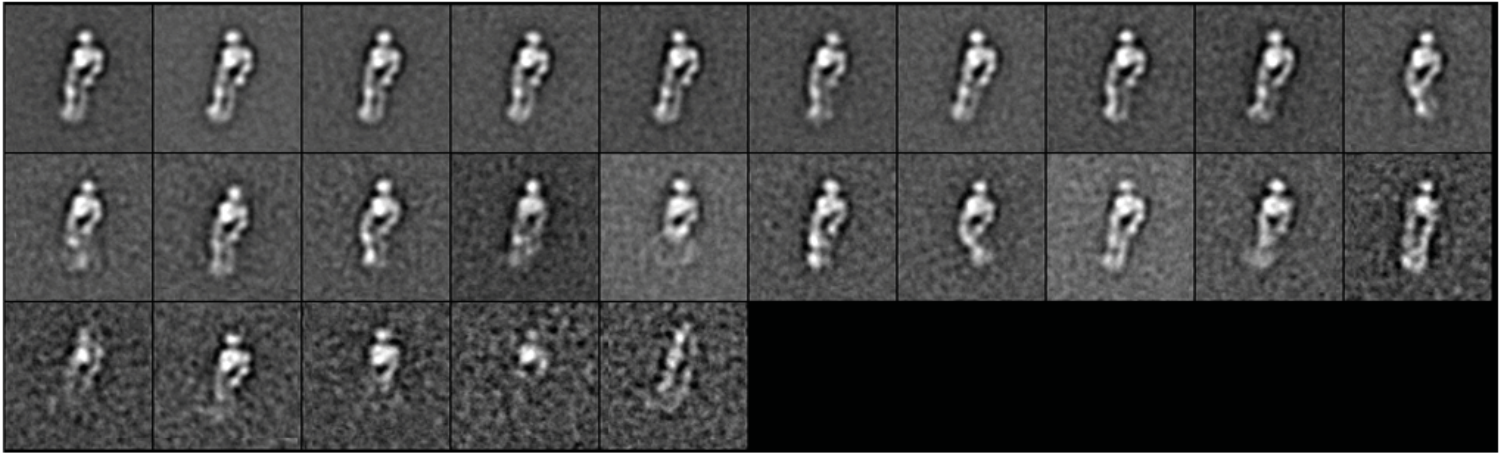


20 nm

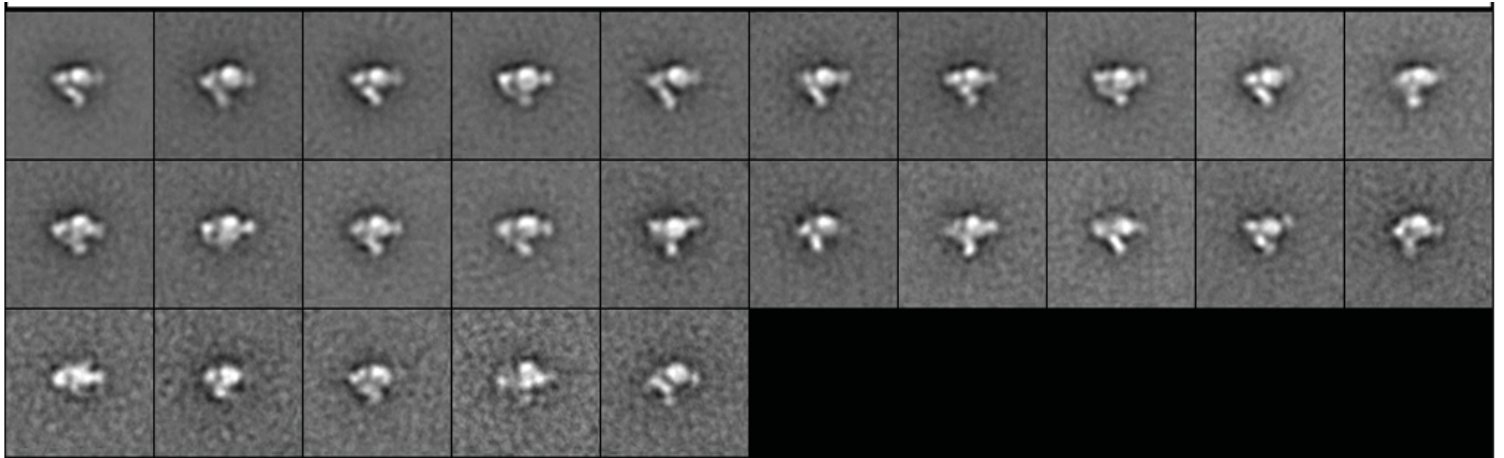
Fig. S2c, d

e Class average of $\alpha_x\beta_2$ (+ CC, - Coil), segregated into extended and bent groups

Extended



Bent



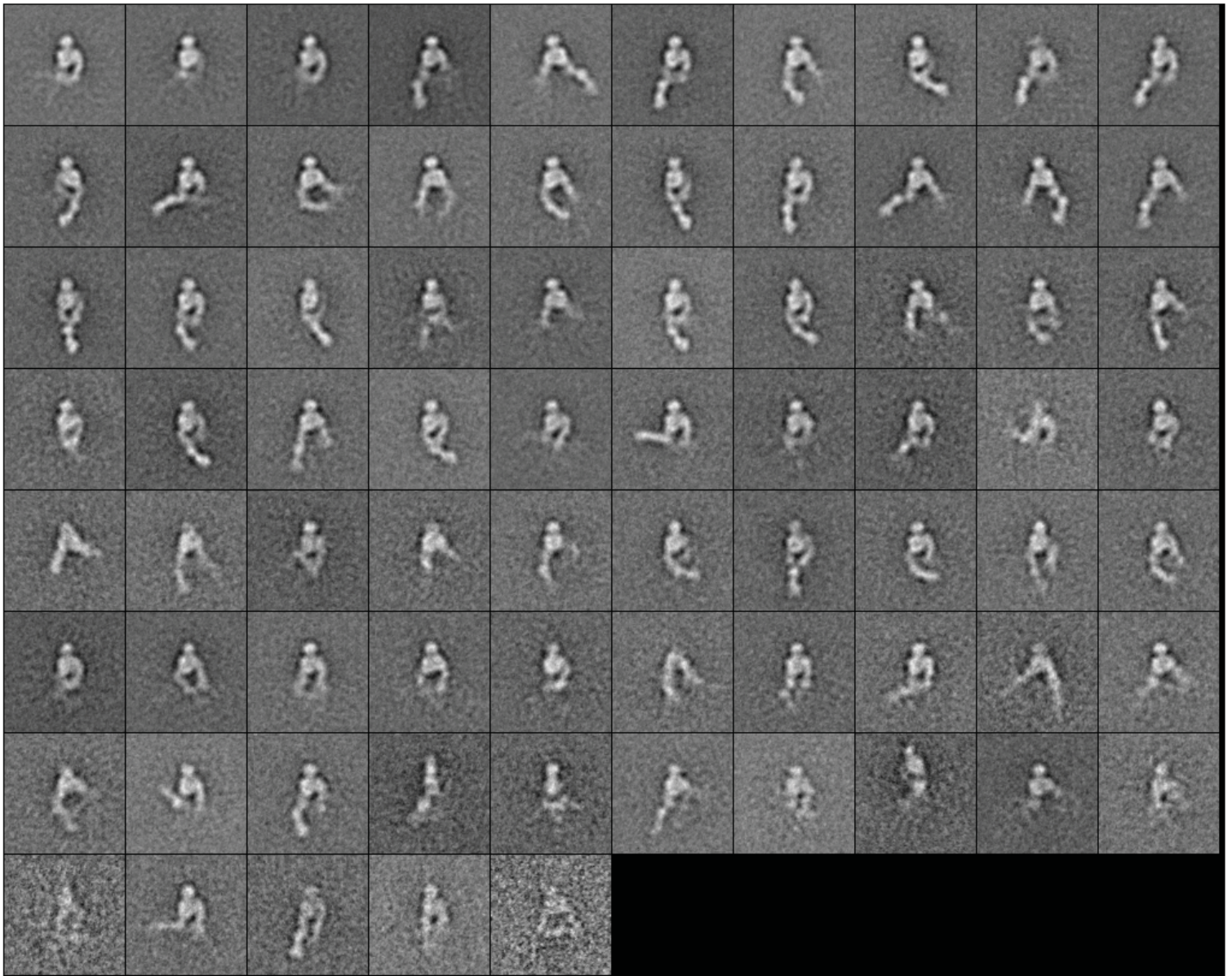
20 nm



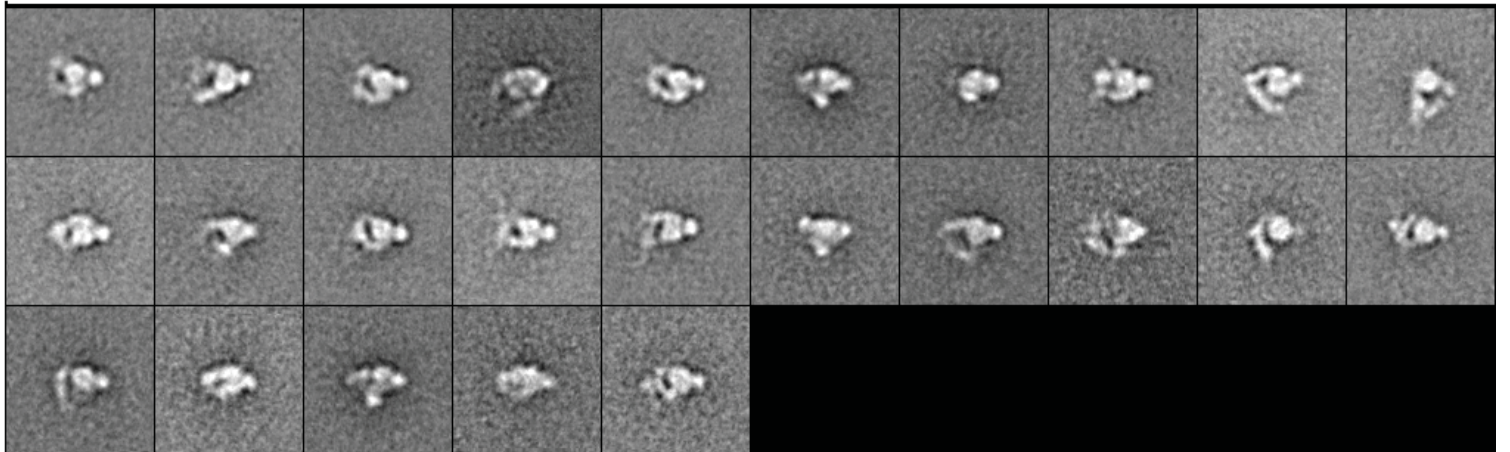
Fig. S2e

f Class average of $\alpha_x\beta_2$ (- CC, - Coil), segregated into extended and bent groups

Extended



Bent



20 nm

Fig. S2f

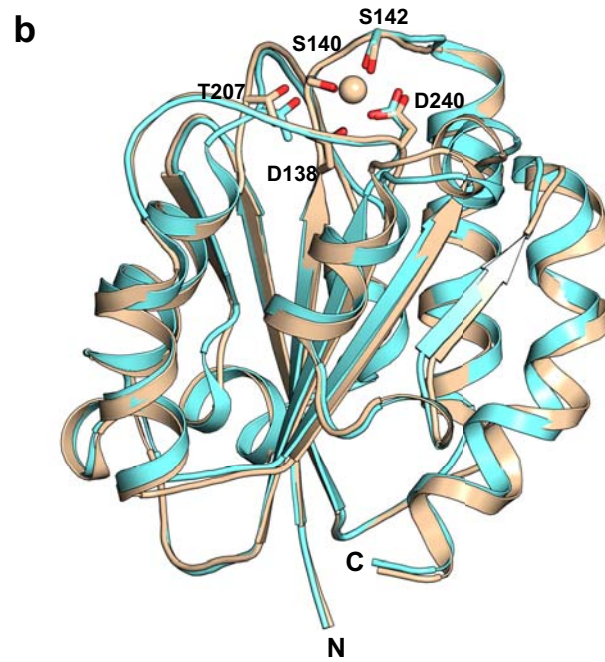
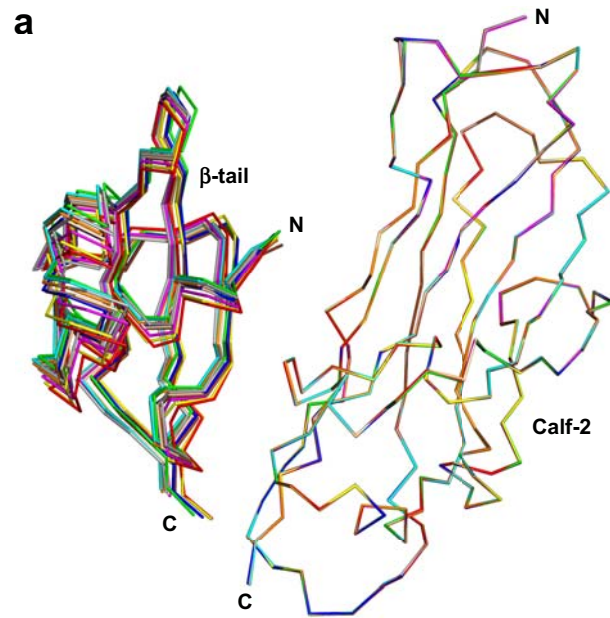


Fig. S3

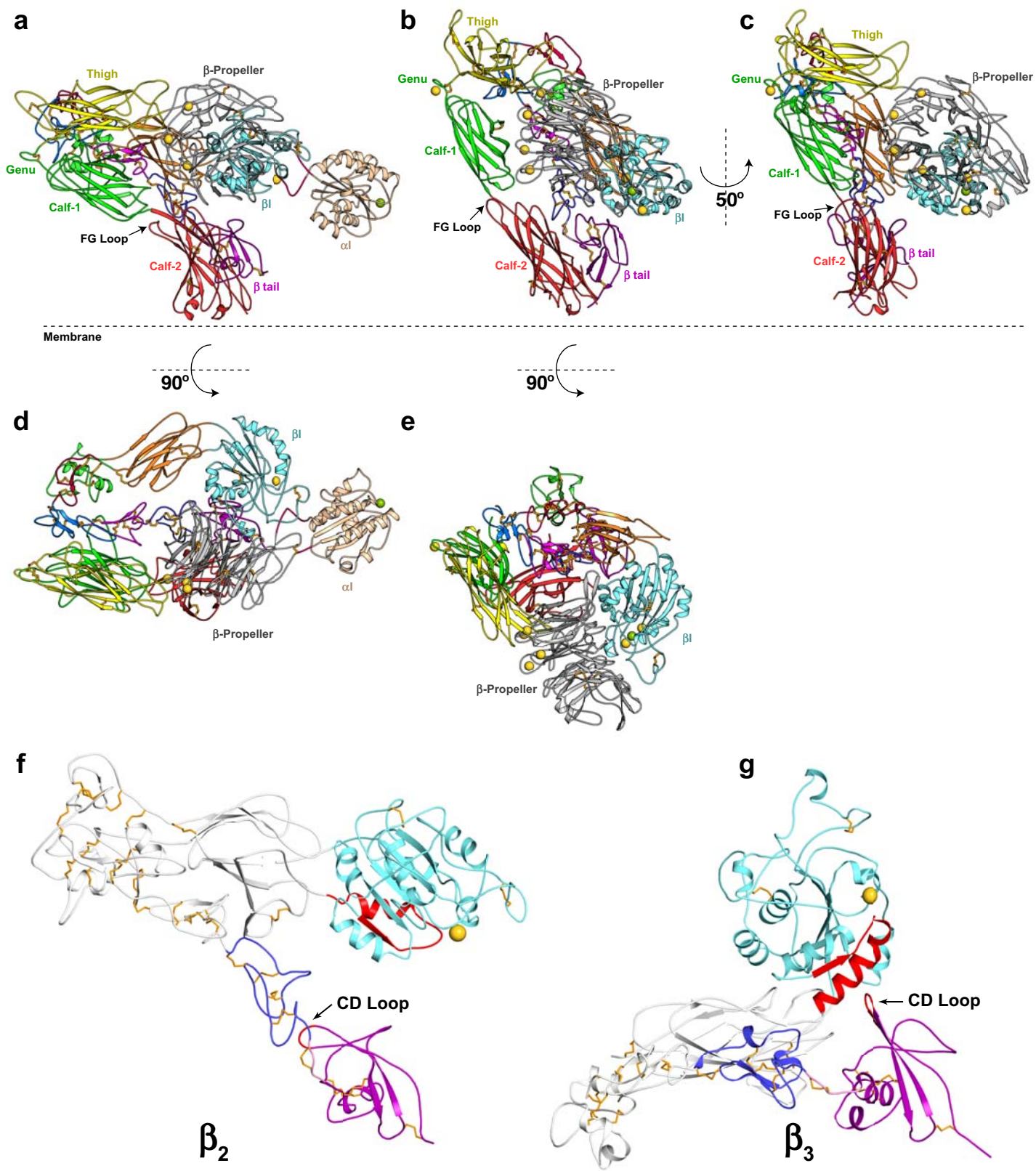


Fig. S4

a

	Thigh	Genu	Calf-1	
α X	YFTASLPFEK- NC GADHIC QD NLGIS-FSFPG	770		
α D	LFTASLPFEK- NC GQDGL CE DLGVT-LSFSG	769		
α M	LFTALFPFEK- NC GNDNIC QD DL SIT-FSFMS	772		
α L	SETWEIPFEK- NC GEDKK CE ANLRVS-FSPAR	764		
α E	FAIFQLPYEK- AC KNKLF CV AELQLA-TTVS-	821		
α 1	SVHEYIPFAK- DC GNKEK CI SDLSLH-VATTE	798		
α 2	AKVFSIPFHK- DC GEDGL CI SDLVLD-VRQIP	778		
α 10	SIQKLVPFK- DC GPDNE CV TDLVLQ-VNMDI	785		
α 11	TLRVSPFWN- GC NEDEH CV PDLVLD-ARSDL	777		
α IIb	HVQEQTRIVL- DC GEDDV CV PQLQLT-ASVT-	619		
α V	NISRQAHILL- DC GEDNV CK PKLEVS-VSD-	613		RGD binding integrins
α 8	IVSEQAHILV- DC GEDNL CV PDLKLS-ARPD-	620		
α 5	RIEDKAQILL- DC GEDN IC VPDQLQLE-VFGE-	621		
α 4	IMKKTINFAR- FC AHEN- CS ADLQVS-AKIGF	606		Fibronectin binding integrins
α 9	AQKNQTVFER- NC RSED- CA ADLQLO-GKLLL	608		
α 3	ENHTEVQFQK- EC GPDNK CE SNLQMR-AAFVS	601		
α 6	TAHIDVHFLKEG CG DDNV CN SNLKLE-YKFCT	621		Laminin binding integrins
α 7	TQRAEIHFLKQ GC GEDK IC QSNLQLVHARFCT	623		

α integrins ↑

↓ α -less integrins

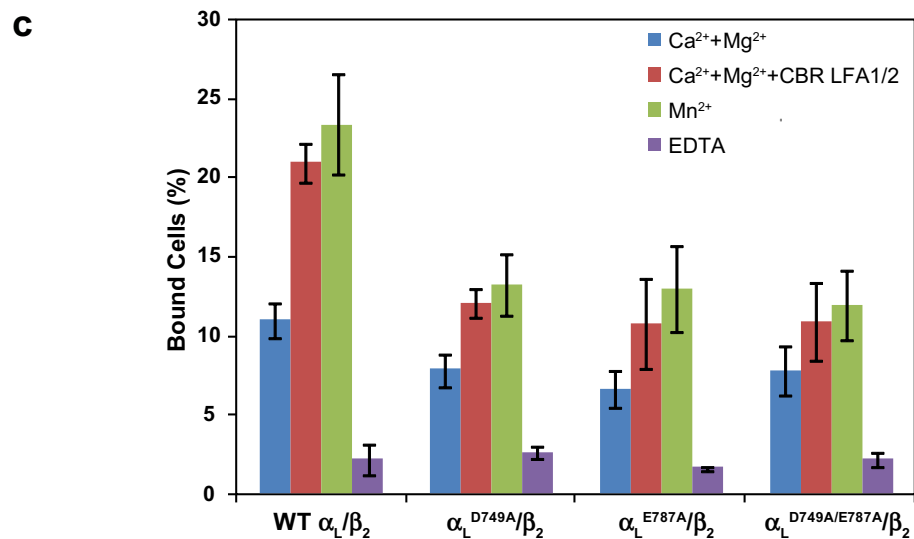
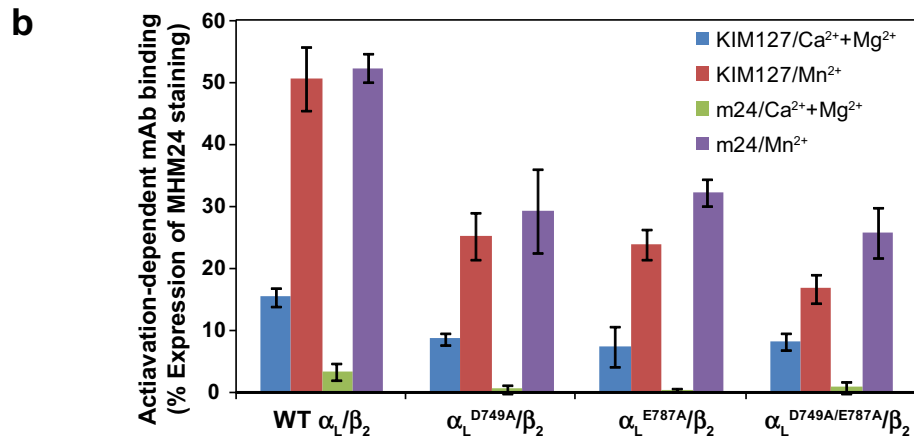



Fig. S5

a

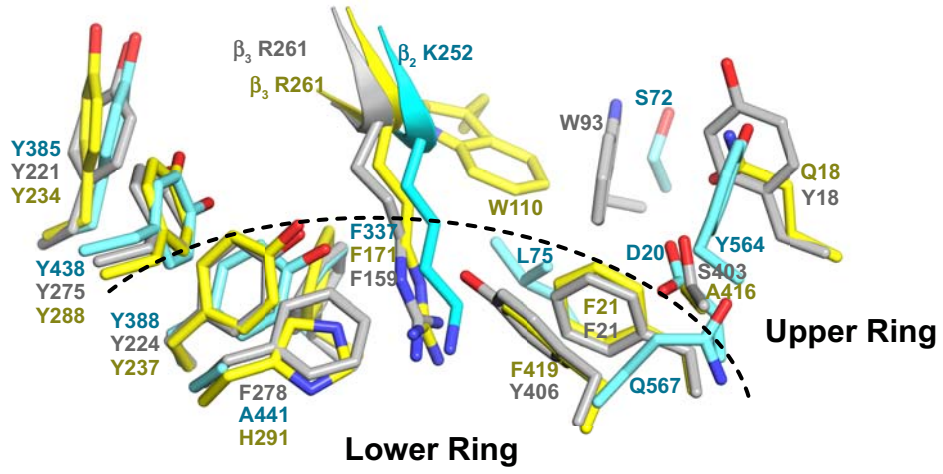
	α I	C-linker	β -Propeller	
				
α X	FDALKDIQNQLKEKIFAIE	EGTETTSSSSFELEMAQ	EGFS	338
α D	FAALGSIQKQLQEKIYAVE	GTQSRASSSFQHEMSQ	EGFS	339
α M	FEALKTIQNQLREKIFAIE	GTQTGSSSSFEHEMSQ	EGFS	340
α L	FEKLDLFTLQKKIYVIE	GTSKQDLTSFNMELSS	SGIS	330
α E	YMALDGLLSKLRYNII	SMEGTV-GD- -ALHYQ	LAQIGFS	388
α 1	ELALVTIVKTLGERIF	AEATADQSAASFEMEM	SQTGFS	356
α 2	EAALLEKAGTLGEQIF	SIEGTVQGGD-NFQME	MSQVGFS	355
α 10	EAALTDIVDALGDRI	FGLGSHAENESSFGL	EMSQIGFS	356
α 11	EAALKDIVDALGDRI	FSLEGTKNET-SFGL	EMSQTGFS	350

b

	Calf2	Transmembrane domain	
α X	QTTTVLEKYKVHNP	TPLIVGSSIGLLLLL	LITAVLY
α M	QTETKVEPF	EVNPLPLIVGSSV	GLLLLLALITAALY
α D	QMEMVLEED	EVYNAIPIIMGSS	VGALLLLALITATLY
α L	VVMKVDVVYEKQ-	MLYLYVLSGIGL	LLLLLLIFIVLY

Fig. S6

a



b

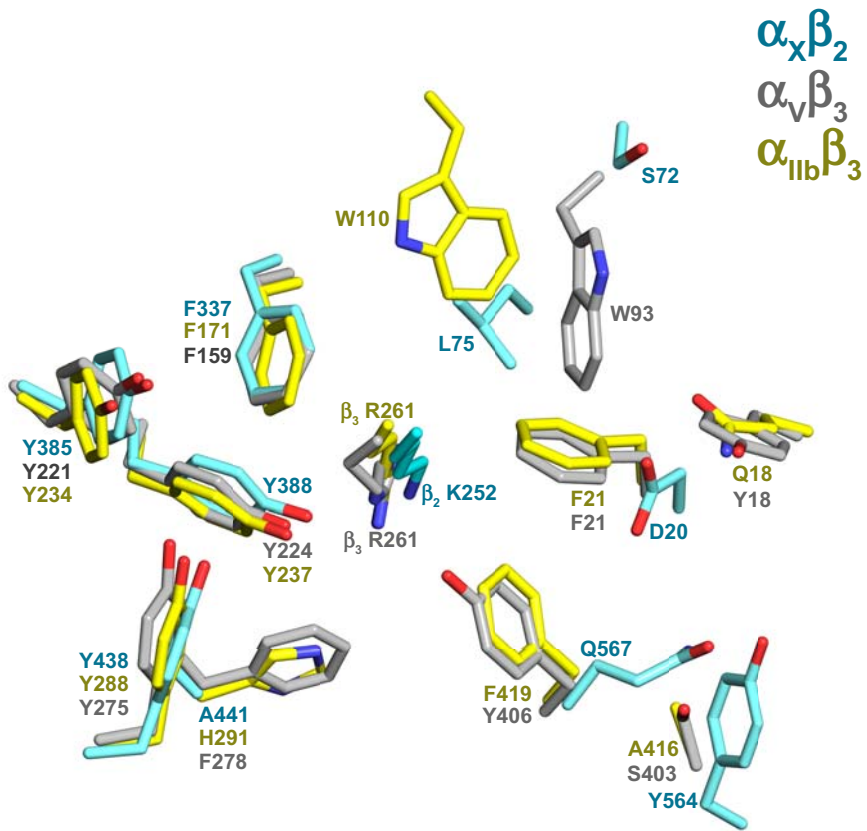


Fig. S7